CRYSTALLOGRAPHIC ORIENTATION ANALYSIS OF FATIGUE CRACK SURFACE FROM AA7050 SAMPLES WITH MULTI-STAGE AGING TREATMENTS

Andre Luis Moreira de Carvalho[1]* and Juliana de Paula Martins[2]

[1]State University of Ponta Grossa, Ponta Grossa, PR, Brazil, [2]Federal University of Technology, Ponta Grossa, PR, Brazil
** Presenting Author email: andrelmc@uepg.br*

Abstract
The microstructure, which contains varying densities of shearable and non-shearable phases resulting from particle-dislocation interactions and microtexture components, contributes to different fatigue crack facet features. In this study, we employed a combination of focused ion beam (FIB) and Electron Back Scatter Diffraction (EBSD) to identify the main components involved in the crack nucleation phase.

1. Introduction

Multiple-stage aging heat treatments have been developed to tailor microstructures in 7000 series Al alloys, producing a good combination of mechanical properties and enhanced corrosion resistance. These properties are influenced by the interaction between precipitates and mobile dislocations in bimodal microstructures containing shearable and shear-resistant precipitates, generated by retrogression and re-aging, as well as interrupted aging heat treatments such as RRA and T6I4 conditions. The microstructure has a strong influence on fatigue crack nucleation and short crack growth via competing mechanisms. This study aims to elucidate the role of microstructure on small fatigue crack crystallography in samples of AA 7050 under RRA, T6I4-65, and T7451 conditions. We used a combination of focused ion beam (FIB) surface preparation and Electron Back Scatter Diffraction (EBSD) to determine fatigue crack surface crystallography near the vicinity of crack initiation sites and within the early crack growth regime.

2. Results

Fatigue crack nucleation sites in alloy 7050 under T6I4-65 and RRA conditions were generated close to clusters of small constituent particles, while for the T7451 condition, nucleation occurred over them. For all three conditions, the fracture surface exhibited a transgranular fracture mode, which is typical of fatigue cracking in this alloy. In the vicinity of the crack initiation sites, a stage I crystallographic fatigue crack growth mode was observed for both T6I4-65 and RRA conditions, but it was absent for the T7451 condition. The fatigue crack facet morphologies during the crack nucleation stage were distinct among the three conditions, with broad-curved-smooth, broad-flat, and broad-rough facets observed for T7451, T6I4-65, and RRA conditions, respectively, and all followed stepped facets. The results shown in Figure 1 display an all-Euler angle (AE) orientation map superimposed on an FIB milled surface for alloy 7050 in the perpendicular regions (L-S plane) close to the fatigue crack nucleation sites, along with corresponding stereographic projection inverse pole-figures indicating the positions of orientation grains obtained on each plane for the three conditions. The cross-section of the Euler space $\Phi 2 = 0°$ and $\Phi 2 = 45°$ was used in the analysis of the orientation distribution function (ODF). Therefore, the main microtexture components from the perpendicular regions (L-S plane) of the crack nucleation sites were $(\bar{1}\bar{1}2)[\bar{1}3\,1]$, $(\bar{1}03)[0\bar{1}0](\bar{3}01)[0\bar{1}0]$ and $(\bar{1}\bar{1}0)[0\bar{1}3]$ orientations for T7451, T6I4-65 and RRA conditions, respectively.

3. Conclusions

Multiple-stage aging heat treatments contribute to the occurrence of stage I crystallographic fatigue crack growth near crack initiation sites, as well as the presence of fatigue crack facet features in the nucleation region due to interactions among different phases, strengthening mechanisms, and microtexture components in T6I4-65 and RRA conditions.

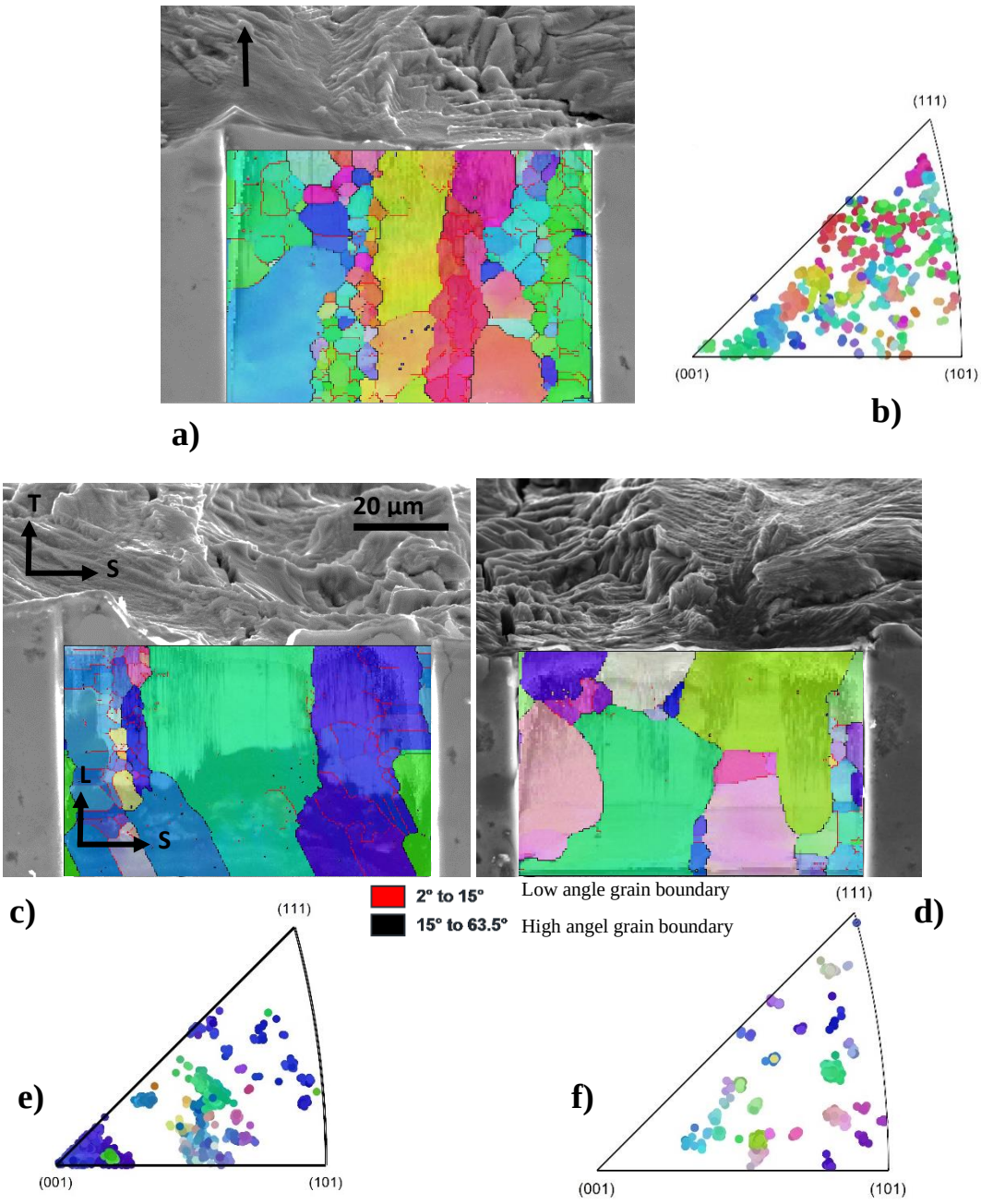

Fig. 1 – SEM images of the fatigue fracture surface of alloy 7050, along with superimposed all-Euler angle (AE) orientation maps on FIB-milled surfaces, are shown for the T7451 (a), T6I4-65 (c), and RRA (d) conditions. Additionally, stereographic projections of the inverse pole-figure showing the positions of orientation grains obtained from EBSD analysis are presented for the T7451 (b), T6I4-65 (e), and RRA (f) conditions. The SEM stage was tilted at an angle of 70° parallel to the S direction, and a black arrow indicates the crack propagation direction.

Acknowledgements

The authors would like to acknowledge the State University of Ponta Grossa's Multiusers Laboratory Complex C-labmu, in collaboration with the Brazilian Nanotechnology National Laboratory Research in Energy and Materials (LNNano-CNPEM), for their support.